



Research article

Inhibitory effect of red LED irradiation on fibroblasts and co-culture of adipose-derived mesenchymal stem cells



Viviane Theodoro^a, Lucas de Oliveira Fujii^a, Leticia Dudri Lucke^b, Fernanda Oriani Bortolazzo^b, Daniela Fernanda Dezotti Silva^a, Giane Daniela Carneiro^b, Maria Esméria Corezola do Amaral^a, Camila Andréa de Oliveira^a, Thiago Antonio Moretti de Andrade^a, André Luis Bombeiro^b, Cristina Pontes Vicente^b, Fernando Russo Costa do Bomfim^a, Alexandre Leite Rodrigues de Oliveira^b, Vanderlei Salvador Bagnato^c, Marcelo Augusto Marretto Esquisatto^a, Fernanda Aparecida Sampaio Mendonça^a, Gláucia Maria Tech dos Santos^a, Andrea Aparecida de Aro^{a,b,*}

^a Biomedical Sciences Graduate Program, University Center of Herminio Ometto Foundation / FHO, Araras, São Paulo, Brazil

^b Department of Structural and Functional Biology, Institute of Biology, State University of Campinas - UNICAMP, Campinas, São Paulo, Brazil

^c Institute of Physics of São Carlos, University of São Paulo – USP, São Carlos, São Paulo, Brazil

ARTICLE INFO

Keywords:

Biological sciences
Cell biology
Proteins
Biomedical engineering
Molecular biology
Regenerative medicine
Scratch assay
Ctgf
TGF- β 1
Tenomodulin
Repair
Cell migration

ABSTRACT

The objective of this study was to evaluate the effects of red Light Emitting Diode (red LED) irradiation on fibroblasts in adipose-derived mesenchymal stem cells (ASC) co-culture on the scratch assay. We hypothesized that red LED irradiation could stimulate paracrine secretion of ASC, contributing to the activation of genes and molecules involved in cell migration and tissue repair. ASC were co-cultured with NIH/3T3 fibroblasts through direct contact and subjected to red LED irradiation (1.45 J/cm²/5min6s) after the scratch assay, during 4 days. Four groups were established: fibroblasts (F), fibroblasts + LED (FL), fibroblasts + ASC (FC) and fibroblasts + LED + ASC (FLC). The analyzes were based on *Ctgf* and *Reck* expression, quantification of collagen types I and III, tenomodulin, VEGF, TGF- β 1, MMP-2 and MMP-9, as well as viability analysis and cell migration. Higher *Ctgf* expression was observed in FC compared to F. Group FC presented higher amount of tenomodulin and VEGF in relation to the other groups. In the cell migration analysis, a higher number of cells was observed in the scratched area of the FC group on the 4th day. There were no differences between groups considering cell viability, *Reck* expression, amount of collagen types I and III, MMP-2 and TGF- β 1, whereas TGF- β 1 was not detected in the FC group and the MMP-9 in none of the groups. Our hypothesis was not supported by the results because the red LED irradiation decreased the healing response of ASC. An inhibitory effect of the LED irradiation associated with ASC co-culture was observed with reduction of the amount of TGF- β 1, VEGF and tenomodulin, possibly involved in the reduced cell migration. In turn, the ASC alone seem to have modulated fibroblast behavior by increasing *Ctgf*, VEGF and tenomodulin, leading to greater cell migration. In conclusion, red LED and ASC therapy can have independent effects on fibroblast wound healing, but the combination of both does not have a synergistic effect. Therefore, future studies with other parameters of red LED associated with ASC should be tested aiming clinical application for tissue repair.

1. Introduction

The wound healing and the repair of other connective tissues like tendon or cartilage, are important though complicated processes that can be impaired by age or by diseases such as diabetes, obesity or

hypertension (Prakash et al., 2016; Phillips et al., 2016; Ho et al., 2017; Goebel et al., 2017; Wang et al., 2018; Yang et al., 2018; Andriolo et al., 2019). The incidence of the connective tissue injuries is high and the treatments for the repair of these tissues present significant financial and resource burden to the health care system (Everts et al., 2017; Ho et al.,

* Corresponding author.

E-mail address: andreaaro80@gmail.com (A.A. de Aro).

<https://doi.org/10.1016/j.heliyon.2020.e03882>

Received 27 January 2020; Received in revised form 27 March 2020; Accepted 27 April 2020

2405-8440/© 2020 Published by Elsevier Ltd. This is an open access article under the CC BY-NC-ND license (<http://creativecommons.org/licenses/by-nc-nd/4.0/>).

2017; Wang et al., 2018; Yang et al., 2018). Thus, strategies that improve the repair of these tissues and mainly improve their functional recovery are of extreme importance.

Phototherapy has been the focus of several studies in the treatment of different adverse health conditions, and Light Emitting Diode (LED) represents a therapeutic option because of its potential in modulating reactions in biological tissues (de Melo et al., 2016). The photons emitted by LED irradiation are absorbed by specific cellular photoreceptors, initiating several intracellular reactions, which lead to changes in membrane potential, O₂ consumption and RNA and DNA synthesis (Prindeze et al., 2012; Avci et al., 2013). These events contribute to the therapeutic effects of LED irradiation demonstrated in the repair of some tissues, such as muscle, skin, tendon, and periodontium (de Melo et al., 2016; Chen et al., 2019; Martignago et al., 2019; Nascimento et al., 2019). Despite benefiting tissue repair, the therapeutic potential of LED irradiation is still controversial due to the divergence of protocols used (Yeh et al., 2010).

In vitro data from Sassoli et al., (2016), show that low intensity 635 nm diode laser irradiation inhibits NIH/3T3 fibroblasts differentiation in myofibroblasts induced by TGF- β 1, decreases expression of type I collagen, upregulates matrix metalloproteinases (MMP)-2 and MMP-9. As for red LED irradiation, it can inhibit fibroblast proliferation in a dose-dependent manner (Lev-Tov et al., 2013) through mitochondrial modulation and other intracellular processes (Mamalis et al., 2016a,b). The visible light may further influence fibroblast migration through the PI3K/Akt and MAPK/ERK pathways (Guo et al., 2010; Choi et al., 2012), or through reactive oxygen species (ROS) levels modulated by the dose of energy used (Mamalis et al., 2015a,b).

Adipose-derived mesenchymal stem cells (ASC) have therapeutic potential in regenerative medicine, and are considered a tool for the replacement of dead or damaged cells, thus contributing to tissue repair or regeneration of tissue (Mazini et al., 2019). They present immunomodulatory and paracrine effects, as well as the ability to differentiate into multiple cell lines (Bacakova et al., 2018; Mazini et al., 2020). During tissue repair, ASC have shown promising effects on the repair of skin, cartilage, bone, muscle, tendon, among many other tissues (Bacakova et al., 2018; de Aro et al., 2018; Gorecka et al., 2018; Frauz et al., 2019; Hamada et al., 2019; Lucke et al., 2019; Paganelli et al., 2019). However, ASC paracrine effects are not completely known.

Considering that phototherapy and cellular therapy with ASC are promising therapeutic modalities for tissue repair, we hypothesized that red LED irradiation could stimulate paracrine secretion of ASC, contributing to the activation of genes and molecules involved in cell migration and tissue repair. Thus, the objective of this study was to evaluate the effects of red LED irradiation on fibroblasts in ASC co-culture in the scratch assay.

2. Materials and methods

2.1. Isolation of ASC and cell culture

Adipose tissue was obtained from the inguinal region of male Wistar rats (n = 6) aged between 90-120 days, obtained from the Animal Experimentation Center (CEA) of the Hermínio Ometto Foundation University Center – FHO/UNIARARAS. The rats were euthanized using anesthetics overdose of Ketamine (270 mg/kg) and Xylazine (36 mg/kg). According to (Yang et al., 2011), with some modifications, adipose tissue was cut and washed in Dulbecco's modified phosphate buffered saline solution (DMPBS Flush, Nutricell Nutrientes Celulares, Campinas, São Paulo, Brazil) containing 2% streptomycin/penicillin. Then, 0.2% collagenase (Sigma- Aldrich® Inc., St. Louis, MO, USA) was added to induce extracellular matrix (ECM) degradation, which is composed by loose connective tissue highly vascularized and innervated, and the solution was maintained at 37 °C under gentle stirring for 1 h to separate the stromal cells from primary adipocytes. Dissociated tissue was filtered using cell strainers (40 μ m) and the inactivation of collagenase was then

done by the addition of an equal volume of Dulbecco's modified Eagle's medium (DMEM) supplemented with 15% fetal bovine serum (FBS), followed by centrifugation at 417 g for 10 min. The suspending portion containing lipid droplets was discarded and the pellet was resuspended in DMEM (containing 50 mg/L penicillin and 50 mg/L streptomycin) with 15% FBS and transferred to 75 cm² bottle, maintained at 37 °C with 5% CO₂ until the 5th passage (5P). ASC were characterized by flow cytometry and cell differentiation assay. The animal procedures were approved by the Animal Use Ethics Committee (CEUA) of the University Center of Hermínio Ometto Foundation - FHO/UNIARARAS, under number 049/2016.

2.2. Flow cytometry for ASC characterization

ASC at 5P were trypsinized and centrifuged at 1,800 rpm for 10 min and counted using the Neubauer chamber. 1×10^6 ASCs were resuspended in 200 μ L of DMPBS Flush with 2% BSA (bovine serum albumin) and the following antibodies were used: CD90-APC (eBioscience®, San Diego, CA, USA), CD105-PE (BD-Pharmingen™, San Diego, CA, USA) and CD45-FITC (eBioscience®, San Diego, CA, USA) (Dominici et al., 2006). Subsequently, ASC were washed twice with 500 μ L of DMPBS Flush and centrifuged at 2,000 rpm for 7 min. The ASCs were resuspended in DMPBS Flush with 2% BSA, following by the flow cytometry analysis.

2.3. *In vitro* osteogenic and adipogenic differentiation of ASC

ASC at 5P (2×10^4) were plated onto 12-wells plate and with ~80% confluency, then were cultured using different mediums for osteogenic (n = 4) and adipogenic differentiation (n = 4). Osteogenic differentiation: DMEM medium supplemented with 8% FBS, 200 μ mol/L of ascorbic acid, 10 mmol/L of β -glycerophosphate and 0.5 μ mol/L of dexamethasone. Adipogenic differentiation: DMEM medium supplemented with 15% FBS, 10 μ g/mL de insulin, 100 μ mol/L de indometacin (Sigma-Aldrich® Inc.) and 1 μ mol/L dexamethasone. The mediums were replaced twice a week, during 30 days, and followed for the Alizarin Red-S (0.2%) and Sudan IV (1%) staining (Caetano et al., 2015).

2.4. Experimental groups and red LED therapy

Four experimental groups were established: F (NIH/3T3 fibroblasts), FL (NIH/3T3 fibroblasts + red LED application), FC (NIH/3T3 fibroblasts + ASC co-culture), and FLC (NIH/3T3 fibroblasts + ASC co-culture + red LED application).

The NIH/3T3 fibroblasts (23–25P) were plated at a density of 1×10^4 per well (for groups F and FL) in 24-well culture plates. Then, the ASC (5P) were added at a density of 5×10^3 (for the FC and FLC groups) per well, followed by incubation with culture medium, DMEM supplemented with 15% FBS, under a humid atmosphere at 37 °C containing 5% CO₂ for cell adhesion. After approximately 70% confluence, the scratch assay was performed using a pipette tip p1000, which was slid all the way through the median well of the previously demarcated well, creating a "scratch" on the cell monolayer. The cultures were washed with DMPBS to remove cell debris and kept in for 24h (for the establishment of the time of LED irradiation) or during 4 days according to the F, FL, FC and FLC groups.

For LED therapy, three different energy densities were analyzed to determine the application dose using the Biotable apparatus (type: Red LED LXM2-PD010040; and source: Luxeon. Equipment developed at the University of São Paulo, São Carlos Institute of Physics, Optics group, Technological Support Laboratory – LAT, São Carlos, SP, Brazil), with a power density of 0.0052 W/cm². Thus, the three energy densities, analyzed by the cell viability test were 0.2 J/cm² for 40s, 1.45 J/cm² for 5min6s and 2.91 J/cm² for 9min33s, 24h after LED irradiation, as a study by Basso et al. (2012). Energy density was calculated by the formula: ENERGY DENSITY = POWER DENSITY (W/cm²) X TIME (s).

As a result of the cell viability test (Figure 2A), the application of the 635 nm red LED irradiation was established at a time of 5min6s. The FL and FLC groups received the application of the red LED irradiation from day 0 to the 3rd day after scratching, followed for collection 24 h after the last application (day 4). The samples were analyzed for cell viability, qRT-PCR, Western blotting and zymography.

2.5. Cell viability assay by MTT test [3-(4,5-dimethylthiazole-2)-2,5-diphenyltetrazolium bromide]

For groups F and FL, NIH/3T3 fibroblasts were plated in sextuplicate at 1×10^4 density per well in 24-well culture plates. Then, for the FC and FLC groups, the ASC were added at a density of 5×10^3 per well and incubated with culture medium under a humid atmosphere at 37 °C containing 5% CO₂ for 24h. After this period, the scratch assay was performed and the cultures were maintained until the 4th day. Control wells were included: 1) only culture medium to be considered as “blank” in absorbance reading; 2) positive controls (Group F) with culture medium and NIH/3T3 fibroblasts (1×10^4 cells per well), used as normalizer for the values of FL, FC and FLC groups; 3) negative controls with 50% DMSO (dimethylsulfoxide) added to the complete culture medium. On the 4th day, after the removal of the complete culture medium from each well, 180 µL DMEM medium without phenol red and 20 µL of 0.5% MTT (Sigma-Aldrich, St. Louis, MO, USA) in DMPBS (5 mg/mL) were added and incubated for 4h protected from light in a 37 °C stove containing 5% CO₂ (Yoshino et al., 2013; Hou et al., 2019). After MTT removal, 200 µL DMSO was added to the wells. The absorbance in each well, including blanks, was measured at 570 nm in a microplate reader. For cell viability calculation, the following formula was used: CELL VIABILITY (%) = (Sample Absorbance/Positive Control Absorbance) x100.

2.6. Quantitative real-time polymerase chain reaction (qRT-PCR)

Each sample was collected from a 24-well plate, totaling 4 samples per group. The RNA extraction was performed using RNeasy Plus Mini Kit, according to the manufacturer's instructions (Qiagen®, cat. code: 74134). RNA concentration was estimated using the Evolution™ 300 UV-VIS spectrophotometer, 260 nm wavelength and SoftwareOrigin® Pro 8. Sample quality was calculated by the absorbance ratio at 260 and 280 nm. From 2µg RNA, cDNA synthesis was performed using the QuantiNova Reverse Transcription kit (Qiagen®, cat. code: 205411).

The qRT-PCR (triplicates) was performed in a thermocycler (Mx3005P, Stratagene) using cDNA (100 ng), QuantiNova SYBR Green PCR kit (Qiagen®, cat. code: 208052) and primers (5 pmol, Table 1); applying the following settings: 1 cycle at 95 °C for 10 min, followed by 40 cycles at 95 °C for 15 s and 60 °C for 1 min. For the relative quantification, we employed the formula $2^{-\Delta\Delta Ct}$ (Winer et al., 1999) with *rplp0* as the reference gene.

2.7. Extraction and dosage of total proteins

For total protein extraction, 50 µL of Tissue Protein Extraction Reagent 78510 - Thermo Fisher Scientific (T-PER™) reagent with protease inhibitor cocktail - 04693159001 SIGMA®) was added at a ratio of 1: 7 to each cell sample (4 samples per group, each from three wells) after trypsinization (Lucke et al., 2019). Then, the samples were homogenized

with sonicator for 90 s in an ice bath. After the centrifugation of the samples at 12,000 rpm and 4 °C for 20 min, the supernatant was collected for protein dosage by the Biuret method (Protal colorimetric method, Laborlab, São Paulo, Brazil), followed by Western blotting and zymography.

2.8. Western blotting

50 µg of each sample were incubated at 100 °C for 5 min in 20% volume of Laemmli Buffer (0.1% bromophenol blue, 1 mol/L sodium phosphate, 50% glycerol, 10% SDS). For electrophoretic race, a volume corresponding to 50 µg of protein in biphasic gel: stacking gel (4 mmol/L EDTA, 2% SDS, 750 mmol/L base Trisma, 6.7 pH) and resolution gel (4 mmol/L EDTA, 2% SDS, 50 mmol/L base Trisma, 6.7 pH). The race was performed at 90 V for approximately 2 h with Running Buffer (200 mmol/L base Trism, 1.52 mol/L glycine, 7.18 mmol/L EDTA and 0.4% SDS), diluted 1:4. Samples were transferred to PVDF membranes (Immun-Blot®; BioRad Laboratories, Inc., Hercules, CA, USA) for 2 h at 120 V on ice, bathed with Transfer Buffer (25 mmol/L base Trism, 192 mmol/L glycine). After transfer, the membranes were blocked with bovine albumin in basal solution for 1:30 h at room temperature. Then, the membranes were washed three times for 10 min with basal solution and incubated overnight under shaking at 4 °C with basal solutions plus 3% serum bovine albumin containing the following primary antibodies: TGF-β1 (transforming growth factor beta-1, sc-52893, 1:200), VEGF (sc-53462, 1:200), collagen I (C2456-Sigma, 1:2,000), collagen III (C7805-Sigma, 1:4,000), tenomodulin (SAB2108237-Sigma, 1:500) and β-actin (sc-47778, Santa Cruz Biotechnology, California, CA, USA, 1:100). Subsequently, the membranes were washed three times for 10 min with basal solution and then incubated under agitation for 2 h in a solution containing the following secondary antibodies: goat anti-mouse IgG1-HRP: sc-2060, 1:1,000 (TGF-β1, VEGF, collagen I, collagen III and β-actin), and mouse anti-rabbit IgG-HRP: sc-2357, 1:10,000 (tenomodulin). Membranes were washed with basal solution and incubated for 1 min with Thermo Scientific®chemiluminescent reagents and exposed to the Syngene photodocumentator (G: BOX) for documentation. The intensity of the bands was evaluated by densitometry through the ImageJ program (NIH, USA).

2.9. Zymography for MMP-2 and MMP-9

Samples from total extract containing 1 µg of proteins were run through polyacrylamide gel electrophoresis (10%) containing 0.1% gelatin, as described in (Aro et al., 2012). After electrophoresis, the gels were washed and stained with Coomassie Brilliant Blue R-250. The intensity of the isoform bands in each group was determined by the ImageJ program (NIH, USA).

2.10. Cell migration assay

Scratch images were documented daily using inverted microscope (Carl Zeiss - Primo Vért) and Microscope Software ZEN 2012 blue edition. Five wells per group were used, and images were captured in 3 regions (one central and two peripheral) of each well, to analyze cell migration towards the scratch. Images were captured on day zero and were used to measure the scratch size (cm) to obtain the mean value (cm) of its length. This average was used to cut the images from the 1st, 2nd, 3rd

Table 1. Primers used in qRT-PCR.

RNA Template	Gene access bank #	Forward primer (5'-3')	Reverse primer (5'-3')
<i>Ctgf</i>	NM_022266.2	CAGGCTGGAGAAGCAGAGTCGT	CTGGTGCAGCCAGAAAGCTCAA
<i>Reck</i>	NM_001107954.1	AGAGGTCAGGCTTTAAACCACTTG	GAACGGAAGCATGGCTAACAC
<i>Rplp0</i>	NM_022402.2	AGGGTCCTGGCTTTGTCTGTGG	AGCTGCAGGAGCAGCAGTGG

Reck (reversion-inducing cysteine-rich protein with Kazal motifs); *Ctgf* (connective tissue growth factor); *Rplp0* (Ribosomal Protein Lateral Stalk Subunit P0).

and 4th days, in order to isolate only cells that migrated to the scratch area. After the photos' standardization, cells were counted only from the scratch area using the ImageJ program (NIH, USA).

2.11. Statistical analysis

Data from the different groups were analyzed using One-way ANOVA (analysis of variance) test, followed by Tukey's test ($p < 0.05$), using GraphPadPrism® software version 3.0 (GraphPad Software, San Diego, CA, USA). The values were represented by the mean \pm standard deviation.

3. Results

3.1. Adipogenic and osteogenic differentiation of ASC

ASC (5P) stained with Sudan IV (1%) and Alizarin Red-S (0.2%) exhibited intracellular lipid droplets and calcium deposition in the extracellular matrix (Figure 1A-C).

3.2. ASC characterization

High expression of CD90 (75.50 ± 2.96) and CD105 (53.77 ± 1.26) markers and low expression of CD45 (37.60 ± 1.80) (Figure 1D-E) were observed.

3.3. Cell viability

To determine the energy density and exposure time of the red LED irradiation, the times of 40s, 5min6s and 9min33s were tested. The cell viability test after 24h of the red LED irradiation showed no significant differences between the different times (Figure 2A). Then, the intermediate energy density setting (1.6 J/cm^2 , 5min6s) was employed in the following experiments.

On the 4th day after the scratch (Figure 2B), no differences in cell viability (NIH/3T3 fibroblasts) were observed between groups (F: 100.00; FL: 98.37 ± 21.19 ; FC: 90.28 ± 10.28 ; and FLC: 85.27 ± 7.28).

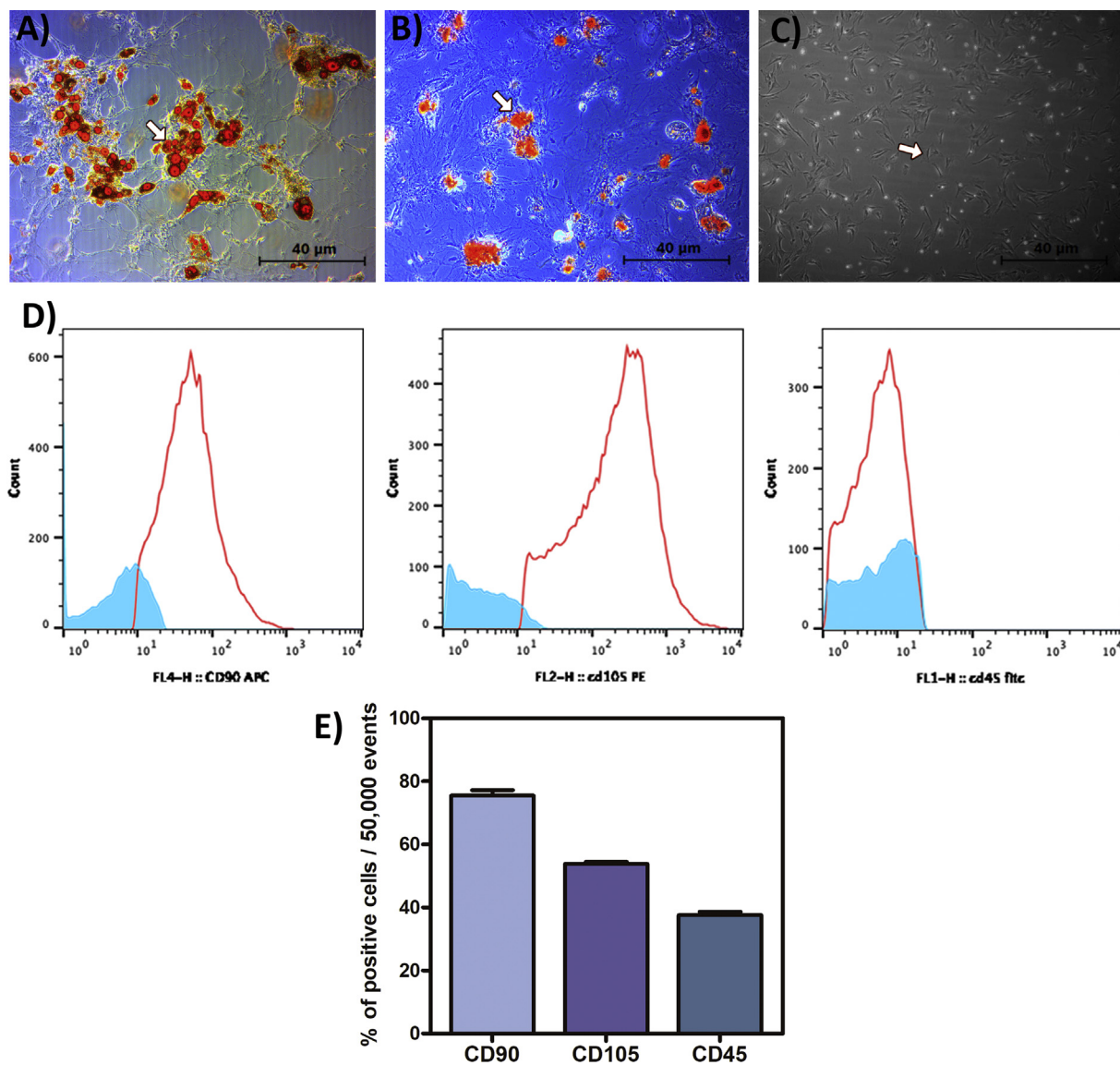


Figure 1. (A) Adipogenic differentiation of ASC (5P) evidenced by intracellular lipid droplets (arrow) stained with Sudan IV, and (B) osteogenic differentiation evidenced by extracellular calcification points (arrow) stained with Alizarin Red-S. (C) Undifferentiated ASC (arrow). (D) Histograms showing the x-axis fluorescence scale considered positive when the cell peak is above 10^1 (CD90), 10^2 (CD 105) or 10^1 (CD45), and controls for -APC, -PE and -FITC, corresponding to non-marked cells due very low fluorescence (in blue). (E) Flow cytometry of ASC (5P): Observe high expression of CD90, CD105 markers and low expression of CD45. Values represented by the mean \pm standard deviation.

3.4. *Reck* and *Ctgf* gene expression

No differences in *Reck* expression were observed between the groups (F: 1.08 ± 0.56 ; FL: 0.90 ± 0.96 ; FC: 1.49 ± 0.86 ; e FLC: 1.05 ± 0.57) (Figure 3). *Ctgf* expression was increased only in FC (10.02 ± 5.45) compared to group F (1.33 ± 1.07) (Figure 3).

3.5. Quantification of TGF- β 1, VEGF, tenomodulin, collagen types I and III

In Figure 4, a higher amount of VEGF was demonstrated by band densitometry in FC (228.2 ± 22.61) compared to F (133.0 ± 17.75), FL (158.7 ± 38.95) and FLC (150.3 ± 32.27). No differences were observed in the amount of TGF- β 1 between F (154.5 ± 38.8), FL (179.7 ± 23.24) and FC (208.6 ± 48.72), being the TGF- β 1 not detected on FLC. Regarding tenomodulin, FC presented higher value (521.5 ± 74.35) when compared to the other groups (F: 169.5 ± 52.52 ; FL: 143.7 ± 34.40 ; e FLC: 250.6 ± 24.70). No differences were observed in the amounts of collagen types I (F: 150.9 ± 24.05 ; FL: 169.0 ± 32.79 ; FC: 157.2 ± 16.84 ; and FLC: 186.4 ± 8.86) and III (F: 184.0 ± 28.68 ; FL: 190.6 ± 22.93 ; FC: 150.4 ± 31.50 ; and FLC: 170.1 ± 29.13) between the groups.

3.6. MMP-2 and MMP-9 activity

For analysis of MMP-2 and MMP-9 (Figure 5A-C), no MMP-9 isoform (latent and active) was observed. Regarding MMP-2, latent (72 kDa) and active (62 kDa) isoforms were observed in all groups analyzed, but with no differences between them.

3.7. Cell migration

No differences between groups were observed on the 1st day (Figure 6A-B). On the 2nd and 3rd days, FC (132.3 ± 44.34 and 214.7 ± 91.71 respectively) had a higher number of cells in the scratch region

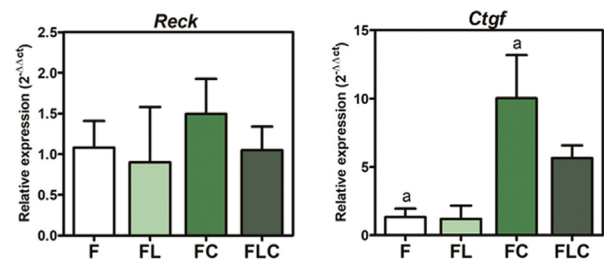


Figure 3. qRT-PCR for *Reck* and *Ctgf* expression: note higher *Ctgf* expression in group FC compared to group F. a = equals letters indicate significant differences between groups ($p < 0.05$). Values represented by the mean \pm standard deviation.

when compared to F (56.0 ± 28.11 and 117.8 ± 73.61) and FL (57.8 ± 32.34 and 115.4 ± 49.98). On the 4th day, the highest number of cells in the scratch region was observed in FC (365.4 ± 103.60) compared to all groups (F: 283.1 ± 100.10 ; FL: 202.3 ± 72.54 ; e FLC: 147.7 ± 51.53), with total scratch closure, followed by group F which presented higher migration compared to groups FL and FLC.

4. Discussion

Our results showed that the red LED irradiation for 5min6s did not alter cell viability, and it decreased cell migration on the 4th day. Kim, Woo et al., (2017) demonstrated a molecular mechanism involved in the stimulatory effect on cell proliferation of LED irradiation (415, 525, 660 and 830 nm), through direct stimulation of the Wnt/ β -catenin and ERK signaling pathway dependent of the energy level (1, 3, 5, or 10 J/cm²). Also, through the increase in the expression of signaling molecules (β -catenin, p-GSK3 β , and Lef1) of the Wnt/ β -catenin pathway after red LED irradiation (655 nm), higher cell proliferation was observed in an *in vitro* culture model (Han et al., 2018). Although speculative, it is possible that the parameters of the LED irradiation used in the present study was not able to activate this signaling pathway, or inhibited it.

Corroborating to our results of cell migration, data from Mamalis et al. (2016) demonstrated that the red LED irradiation (633 nm) inhibited the speed of fibroblast migration *in vitro*, through modulation of the phosphoinositide 3-kinase (PI3K)/Akt pathway. In other study, it was showed that blue LED inhibited adult human skin dermal fibroblast migration speed, and this effect was associated with increased ROS generation in a dose-dependent manner (Mamalis et al., 2015). Green LED (530 nm) irradiation directed the human orbital fat stem cells to migrate away from the LED light source through activation of extracellular signal-regulated kinases (ERK)/MAP kinase/p38 signaling pathway (Ong et al., 2013). In addition, blue LED had an inhibitory effect on migration of cancer cells via phosphorylation of p38 MAPK *in vitro* and *in vivo*, with involvement of MMP-2 and MMP-9 inhibition (Oh et al., 2017). Our data did not show differences in the amount of MMP-2 after red LED irradiation in both FL and FLC groups, excluding the participation of this enzyme involved in the phosphorylation of p38 MAPK. In contrast, the literature reports the promising effect of red LED irradiation (0.5–50 J/cm² of energy density) on the healing processes due to its role in increasing cell viability and proliferation, including fibroblasts (Vincek et al., 2003; Volpato et al., 2011; Teuschl et al., 2015; Oliveira et al., 2016). According to Fushimi et al., (2012), LED promotes wound healing by inducing migratory and proliferative mediators, especially leptin, IL-8 and VEGF. Although the literature describes several molecular signaling pathways, our data does not allow us to describe the signaling pathways possibly inactivated by the effects of red LED irradiation during cell migration. But as described below, it is possible to indicate the participation of *Ctgf* and TGF- β 1.

Our data demonstrated that the LED irradiation may have inhibited fibroblast signaling-induced differentiation of the ASC, since no tenomodulin was observed in the FLC group (Schneider et al., 2011).

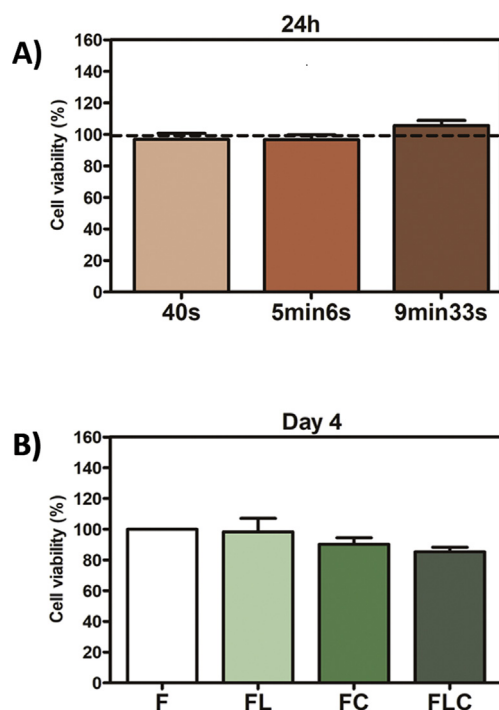


Figure 2. (A) Cell viability analysis of FL group 24h after application of 3 different times: 40s, 5min6s and 9min33s. Observe no differences between the times analyzed. Dashed line represents positive control (B) On the 4th day after the scratch, no differences were observed between the groups. Values represented by the mean \pm standard deviation.

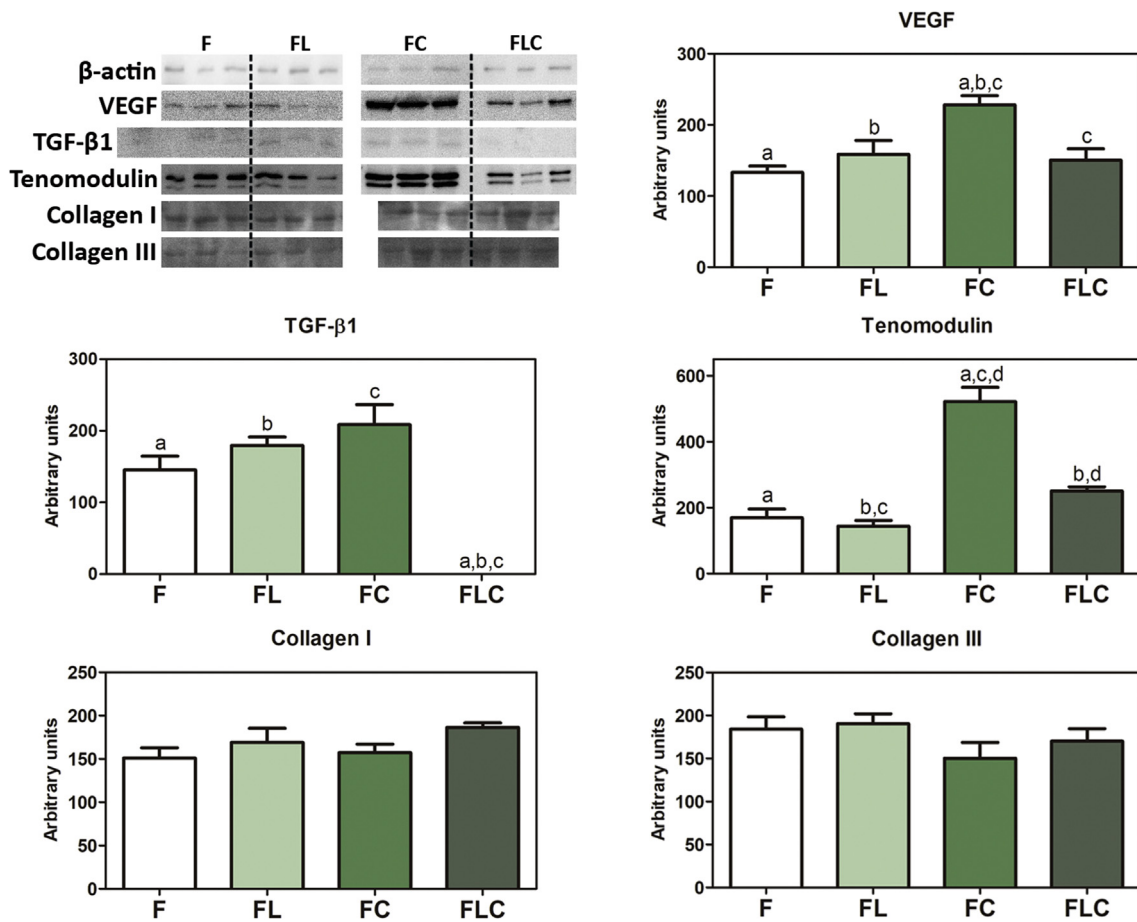


Figure 4. Western blotting and band densitometry for VEGF, TGF-β1, tenomodulin and collagen types I and III. a, b, c, d = equal letters indicate significant differences between the groups ($p < 0.05$). Values represented by mean \pm standard deviation (see supplemental data).

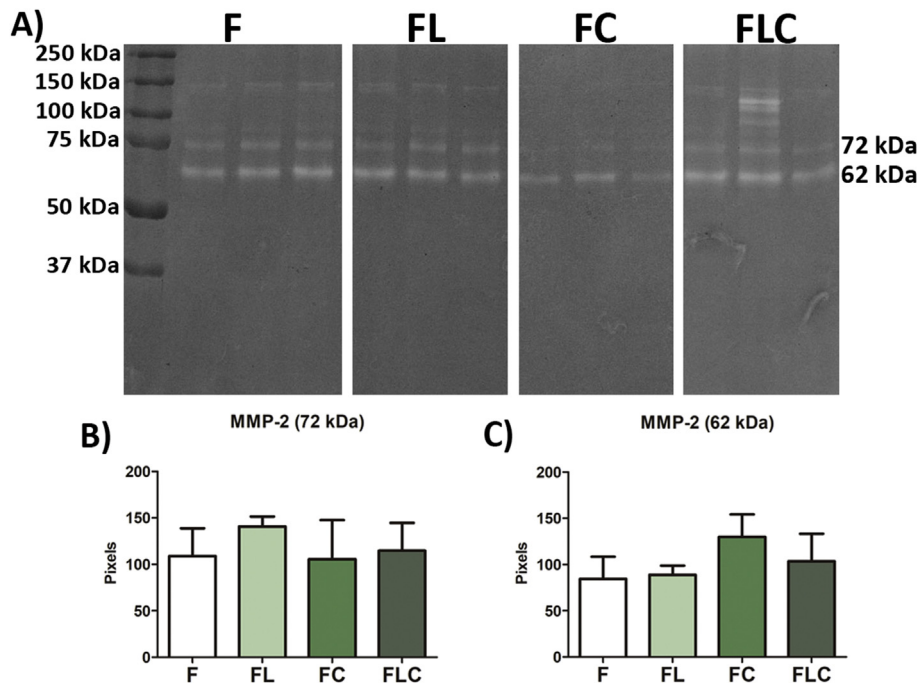


Figure 5. Zymography for MMP-9 and MMP-2: note the absence of MMP-9 and the presence of latent (72 kDa) and active (62 kDa) isoforms of MMP-2 (A). Band densitometry represented in the graphics (B and C), showing no differences between groups. Values represented by mean \pm standard deviation.

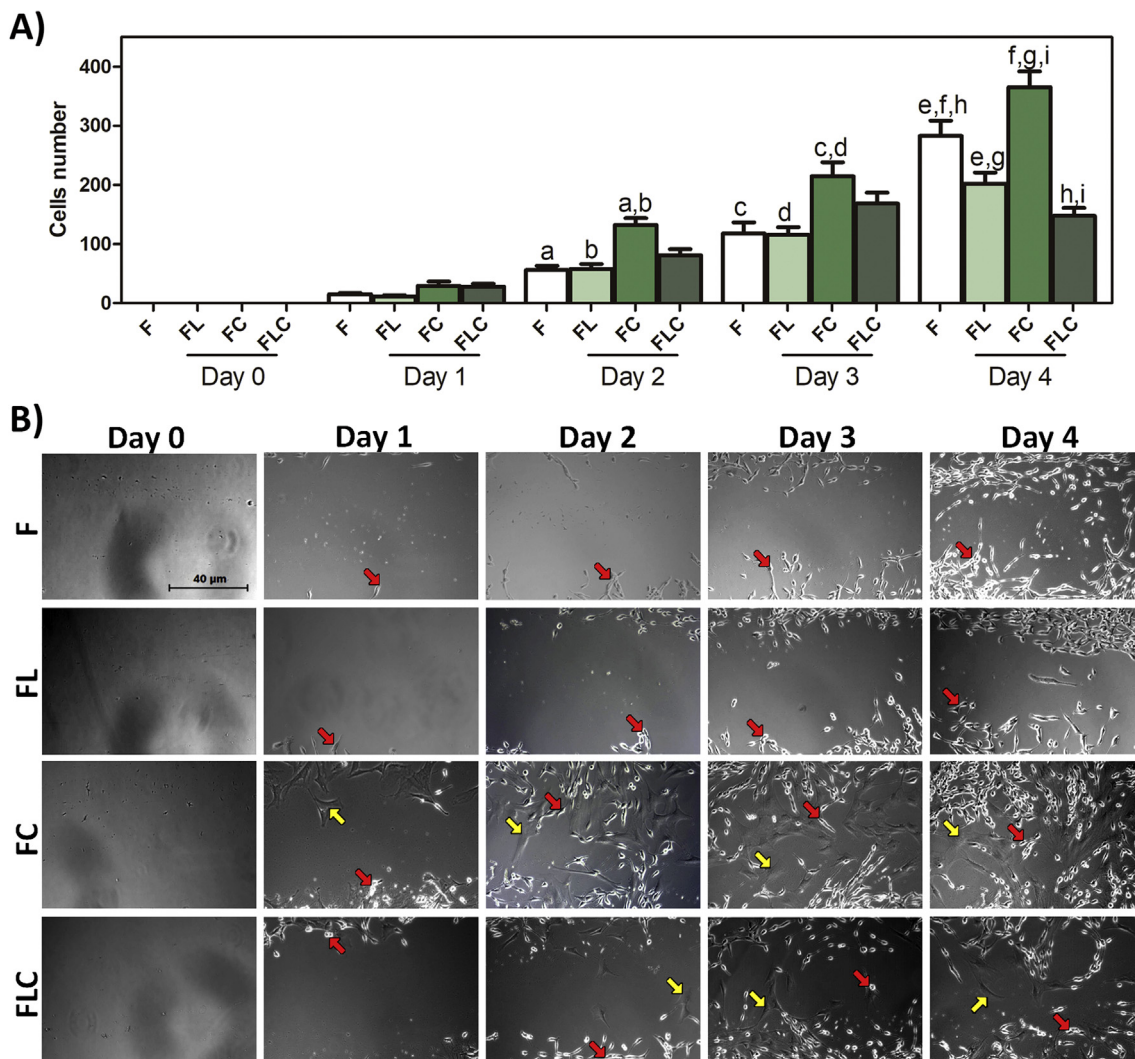


Figure 6. (A) Cell migration analysis: scratch cell count. Note a marked difference for the FC group between the 2nd and 4th days, in relation to groups F, FL and FLC. a, b, c, d, e, f, g, h, i = equal letters represent significant differences between groups ($p < 0.05$). Values represented by the mean \pm standard deviation. (B) Representative images of cell migration for scratch closure on days 0, 1, 2, 3 and 4 of all groups. Migration of NIH/3T3 fibroblasts (red arrow) and ASC (yellow arrow) in the FC and FLC groups. Note that the FC group presented higher migration between the 2nd and 4th days compared to the other groups, with total scratch closure. In addition, a lower amount of ASC was observed in the scratch region in the FLC group compared to the FC group between the 2nd and 4th days.

Tenomodulin is a type II transmembrane glycoprotein used as a cell marker of tenocytes (Shukunami et al., 2006), which also acts on type I collagen fibrillogenesis (Dex et al., 2017). Tenomodulin may also act in the control of cell differentiation and stemness (Morikawa et al., 2016). Though no inhibitory mechanism was demonstrated by Peng et al., (2012), this study corroborates our results because showed no action of red LED on differentiation induction of a kind of mesenchymal stem cells (bone marrow stem cells) in normal media.

Regarding fibroblasts in direct ASC co-culture, total scratch closure was observed on the 4th day, due to the modulating effect of ASC which favored cell migration. Corroborating our findings, *in vitro* studies have shown that ASC increase the migration of keratinocytes, fibroblasts and vascular endothelial cells (Moon et al., 2012; Hu et al., 2013; Zhao et al., 2013; Ferreira et al., 2017). Data from Kim et al., (2007) demonstrated the effects of conditioned medium of ASC on increased migration of human dermal fibroblasts in the *in vitro* healing model, as well as in reducing wound size in *in vivo* healing model. Possible signaling pathways can be involved in the largest cell migration observed in our results due to ASC co-culture. These signaling pathways can be regulated by Reck (Mahl et al., 2016), as for the Fibromodulin (FMDO)-TGF β 1-MMP-2 and FMDO-TGF β 1-CTGF (Zheng et al., 2017). Considering there was no

difference between the groups F, FL and FC regarding the expression of Reck, TGF- β 1 and MMP-2, our data point to the possible involvement of the FMDO-TGF β 1-CTGF pathway, due to the higher *Ctgf* expression in the FC group. With the combination of the LED and the ASC co-culture, there was a marked decrease in cell migration compared to the FC group, indicating that the LED irradiation interfered on the action of ASC.

Our results showed no effect of the red LED irradiation and of the ASC alone on the amount of TGF- β 1, corroborating to no variation in the amount of collagen types I and III. In contrast, a study of Tafinski et al., (2014) using blue LED (420 nm) showed that the TGF- β 1 amount was significantly inhibited after irradiation. TGF- β 1 is a central modulator also during proliferation and tissue healing processes, also stimulating the deposition of major ECM molecules, such as some types of collagen (Morikawa et al., 2016). Proffen, Haslauer et al., (2013) observed that mesenchymal stem cells from the retroperitoneal fat pad in swine anterior cruciate ligament fibroblasts co-culture stimulated gene expression of collagen *in vitro*. Kim, Park et al., (2007) demonstrated that human dermal fibroblasts grown in ASC conditioned medium showed increased expression of collagen types I and III. Regarding the effects of LED application on collagen content, the literature describes inhibitory and stimulatory effects of LED. Huang, Huang et al., (2007) demonstrated

that the red LED irradiation (625–635 nm) stimulated collagen synthesis in fibroblast culture. Studies by Mamalis et al., (2016) and Mamalis and Jagdeo (2017) showed that red LED irradiation (633nm) inhibited collagen production *in vitro*. When associated the ASC co-culture and the red LED irradiation, surprisingly TGF- β 1 was not detected, indicating another molecule for stimulation of collagen synthesis in the FC group, since the amount of collagen types I and III remained similar to other groups.

A higher amount of VEGF was observed in the FC group in relation to the other groups. Corroborating to our findings, studies describe the role of ASC in angiogenesis through VEGF secretion (Robering et al., 2018; Beugels et al., 2019). When red LED irradiation was associated with ASC, our data showed a lower amount of VEGF indicating that LED decreased the vascular potential of ASC. Zhang, Xiong et al., (2009) also demonstrated that red LED irradiation (650 nm) attenuated the elevation of VEGF expression in HeLa cell implanted BALB/c mice. However, data from Priglinger et al., (2018) using the red LED irradiation, although with different parameters than that used in the present work, demonstrated its beneficial effects on the vascularization potential of stromal vascular fraction (SVF), the heterogeneous cell population including the ASC.

The literature is contradictory regarding the biological effects of the red LED irradiation because of different parameters that were employed, such as the energy density and of cell type (Vinck et al., 2003; Huang et al., 2007; Zhang et al., 2009; Volpato et al., 2011; Fushimi et al., 2012; Peng et al., 2012; Teuschl et al., 2015; Oliveira et al., 2016; Mamalis et al., 2016; Kim et al., 2017; Mamalis and Jagdeo, 2017; Han et al., 2018). In the present study, considering that no differences were observed in the cell viability using 0.2, 1.45 and 2.91 J/cm², an intermediate energy density of 1.45 J/cm² was used. A stimulatory response of the LED was expected especially in the ASC co-culture, since some studies demonstrate beneficial effects of red LED with energy density between 0.5–50 J/cm² (Vinck et al., 2003; Volpato et al., 2011; Teuschl et al., 2015; Oliveira et al., 2016). However, our hypothesis was not supported by the results because the red LED irradiation decreased the healing response of ASC. An inhibitory effect of the LED irradiation associated with ASC co-culture was observed due the reduction of the amount of TGF- β 1, VEGF and tenomodulin, possibly involved in the reduced cell migration. In turn, the ASC alone seem to have modulated fibroblast behavior by increasing *Ctgf*, VEGF and tenomodulin, leading to greater cell migration. Still aiming to show a stimulatory LED irradiation effect, other red LED energy densities were not tested and may be considered a limitation of the present study.

In conclusion, red LED and ASC therapy can have independent effects on fibroblast wound healing, but the combination of both does not have a synergistic effect. Therefore, future studies with other parameters of red LED associated with ASC should be tested aiming clinical application for tissue repair.

Declarations

Author contribution statement

A. de Aro and V. Theodoro: Conceived and designed the experiments; Performed the experiments; Analyzed and interpreted the data; Wrote the paper.

G. Santos: Conceived and designed the experiments; Analyzed and interpreted the data; Wrote the paper.

F. Bomfim Conceived and designed the experiments. L. Fujii, F. Bortolazzo, D. Dezotti, G. Carneiro, M. Amaral, C. Oliveira and C. Vicente: Performed the experiments.

L. Lucke: Performed the experiments; Analyzed and interpreted the data; Wrote the paper.

A. Bombeiro: Performed the experiments; Analyzed and interpreted the data.

F. Mendonça: Analyzed and interpreted the data.

T. Andrade, A. Oliveira, V. Bagnato and M. Esquisatto: Contributed reagents, materials, analysis tools or data.

Funding statement

V. Theodoro was supported by Institutional of the University Center of Herminio Ometto Foundation (356/2016).

Competing interest statement

The authors declare no conflict of interest.

Additional information

Supplementary content related to this article has been published online at <https://doi.org/10.1016/j.heliyon.2020.e03882>.

Acknowledgements

The authors would like to thank the Biomedical Sciences Graduate Program of the University Center of Herminio Ometto Foundation/FHO for the support of research, and Daniella N. R. Neodini for technical assistance during Western blotting analysis.

References

- Andriolo, L., Candrian, C., Papio, T., Cavicchioli, A., Perdisa, F., Filardo, G., 2019. Osteochondritis dissecans of the knee - conservative treatment strategies: a systematic review. *Cartilage* 10 (3), 267–277.
- Aro, A.A., Nishan, U., Perez, M.O., Rodrigues, R.A., Foglio, M.A., Carvalho, J.E., Gomes, L., Vidal, B.C., Pimentel, E.R., 2012. Structural and biochemical alterations during the healing process of tendons treated with Aloe vera. *Life Sci.* 91 (17–18), 885–893.
- Avci, P., Gupta, A., Sadasivam, M., Vecchio, D., Pam, Z., Pam, N., Hamblin, M.R., 2013. Low-level laser (light) therapy (LLLT) in skin: stimulating, healing, restoring. *Semin. Cutan. Med. Surg.* 32 (1), 41–52.
- Bacakova, L., Zarubova, J., Travnickova, M., Musilkova, J., Pajorova, J., Slepicka, P., Kasalkova, N.S., Svorcik, V., Kolska, Z., Motarjemi, H., Molitor, M., 2018. Stem cells: their source, potency and use in regenerative therapies with focus on adipose-derived stem cells - a review. *Biotechnol. Adv.* 36 (4), 1111–1126.
- Basso, F.G., Pansani, T.N., Turrioni, A.P., Bagnato, V.S., Hebling, J., de Souza Costa, C.A., 2012. In vitro wound healing improvement by low-level laser therapy application in cultured gingival fibroblasts. *Int. J. Dent.* 2012, 719452.
- Beugels, J., Molin, D.G.M., Ophelders, D.R.M.G., Rutten, T., Kessels, L., Kloosterboer, N., Grzymala, A.A.P., Kramer, B.W.W., van der Hulst, R.R.W.J., Wolfs, T.G.A.M., 2019. Electrical stimulation promotes the angiogenic potential of adipose-derived stem cells. *Sci. Rep.* 9 (1), 12076.
- Caetano, G.F., Bártolo, P.J., Domingos, M., Oliveira, C.C., Leite, M.N., Frade, M.A., C., 2015. Osteogenic differentiation of adipose-derived mesenchymal stem cells into Polycaprolactone (PCL) scaffold. *Procedia Eng.* 110, 59–66.
- Chen, Y.W., Hsieh, O., Chen, Y.A., Chiou, L.L., Chang, P.C., 2019. Randomized controlled clinical effectiveness of adjunct 660-nm light-emitting diode irradiation during non-surgical periodontal therapy. *J. Formos. Med. Assoc.* 119 (1 Pt 1), 157–163.
- Choi, H., Lim, W., Kim, I., Kim, J., Ko, Y., Kwon, H., Kim, S., Kabir, K.M., Li, X., Kim, O., Lee, Y., 2012. Inflammatory cytokines are suppressed by light-emitting diode irradiation of P. gingivalis LPS-treated human gingival fibroblasts: inflammatory cytokine changes by LED irradiation. *Laser Med. Sci.* 27 (2), 459–467.
- de Aro, A.A., Carneiro, G.D., Teodoro, L.F.R., da Veiga, F.C., Ferrucci, D.L., Simões, G.F., Simões, P.W., Alvares, L.E., de Oliveira, A.L.R., Vicente, C.P., Gomes, C.P., Pesquero, J.B., Esquisatto, M.A.M., de Campos Vidal, B., Pimentel, E.R., 2018. Injured achilles tendons treated with adipose-derived stem cells transplantation and GDF-5. *Cells* 7 (9), E127.
- de Melo, C.A., Alves, A.N., Terena, S.M., Fernandes, K.P., Nunes, F.D., da Silva, D. de F., Bussadori, S.K., Deana, A.M., Mesquita-Ferrari, R.A., 2016. Light-emitting diode therapy increases collagen deposition during the repair process of skeletal muscle. *Laser Med. Sci.* 31 (3), 531–538.
- Dex, S., Alberton, P., Willkomm, L., Söllradl, T., Bago, S., Milz, S., Shakibaie, M., Ignatius, A., Bloch, W., Clausen-Schaumann, H., Shukunami, C., Schieker, M., Docheva, D., 2017. Tenomodulin is required for tendon endurance running and collagen I fibril adaptation to mechanical load. *EBioMedicine* 20, 240–254.
- Dominici, M., Le Blanc, K., Mueller, I., Slaper-Cortenbach, I., Marini, F., Krause, D., Deans, R., Keating, A., Prockop, D., Horwitz, E., 2006. Minimal criteria for defining multipotent mesenchymal stromal cells. The International Society for Cellular Therapy position statement. *Cytotherapy* 8 (4), 315–317.
- Everts, P.A., Warbout, M., de Veth, D., Cirkel, M., Spruijt, N.E., Buth, J., 2017. Use of epidermal skin grafts in chronic wounds: a case series. *Int. Wound J.* 14 (6), 1213–1218.

- Ferreira, A.D.F., Cunha, P.D.S., Carregal, V.M., da Silva, P.C., de Miranda, M.C., Kunrath-Lima, M., de Melo, M.I.A., Faraco, C.C.F., Barbosa, J.L., Frezard, F., Resende, V., Rodrigues, M.A., de Goes, A.M., Gomes, D.A., 2017. Extracellular vesicles from adipose-derived mesenchymal stem/stromal cells accelerate migration and activate AKT pathway in human keratinocytes and fibroblasts independently of miR-205 activity. *Stem Cell. Int.* 2017, 9841035.
- Frauz, K., Teodoro, L.F.R., Carneiro, G.D., Cristina da Veiga, F., Lopes Ferrucci, D., Luis Bombeiro, A., Waleska Simões, P., Elvira Álvares, L., Leite R de Oliveira, A., Pontes Vicente, C., Seabra Ferreira, R., Barraviera, B., do Amaral, M.E.C., Augusto M Esquisatto, M., de Campos Vidal, B., Rosa Pimentel, E., Aparecida de Aro, A., 2019. Transsected tendon treated with a new fibrin sealant alone or associated with adipose-derived stem cells. *Cells* 8 (1), E56.
- Fushimi, T., Inui, S., Nakajima, T., Ogasawara, M., Hosokawa, K., Itami, S., 2012. Green light emitting diodes accelerate wound healing: characterization of the effect and its molecular basis in vitro and in vivo. *Wound Repair Regen.* 20 (2), 226–235.
- Goebel, L., Reinhard, J., Madry, H., 2017. Meniscal lesion. A pre-osteoarthritic condition of the knee joint. *Orthopä* 46 (10), 822–830.
- Gorecka, A., Salemi, S., Haralampieva, D., Moalli, F., Stroka, D., Candinas, D., Eberli, D., Brügger, L., 2018. Autologous transplantation of adipose-derived stem cells improves functional recovery of skeletal muscle without direct participation in new myofiber formation. *Stem Cell Res. Ther.* 9 (1), 195.
- Guo, A., Song, B., Reid, B., Gu, Y., Forrester, J.V., Jahoda, C.A., Zhao, M., 2010. Effects of physiological electric fields on migration of human dermal fibroblasts. *J. Invest. Dermatol.* 130 (9), 2320–2327.
- Hamada, T., Matsubara, H., Yoshida, Y., Ugaji, S., Nomura, I., Tsuchiya, H., 2019. Autologous adipose-derived stem cell transplantation enhances healing of wound with exposed bone in a rat model. *PLoS One* 14 (5), e0214106.
- Han, L., Liu, B., Chen, X., Chen, H., Deng, W., Yang, C., Ji, B., Wan, M., 2018. Activation of Wnt/ β -catenin signaling is involved in hair growth-promoting effect of 655-nm red light and LED in in vitro culture model. *Laser Med. Sci.* 33 (3), 637–645.
- Ho, G., Tantigate, D., Kirschenbaum, J., Greisberg, J.K., Vosseller, J.T., 2017. Increasing age in Achilles rupture patients over time. *Injury* 48 (7), 1701–1709.
- Hou, L., Wang, R., Wei, H., Li, S., Liu, L., Lu, X., Yu, H., Liu, Z., 2019. ABT737 enhances ovarian cancer cells sensitivity to cisplatin through regulation of mitochondrial fission via Sirt3 activation. *Life Sci.* 1 (232), 116561.
- Hu, L., Zhao, J., Liu, J., Gong, N., Chen, L., 2013. Effects of adipose stem cell-conditioned medium on the migration of vascular endothelial cells, fibroblasts and keratinocytes. *Exp. Ther. Med.* 5 (3), 701–706.
- Huang, P.J., Huang, Y.C., Su, M.F., Yang, T.Y., Huang, J.R., Jiang, C.P., 2007. In vitro observations on the influence of copper peptide aids for the LED photoradiation of fibroblast collagen synthesis. *Photomed. Laser Surg.* 25 (3), 183–190.
- Kim, W.S., Park, B.S., Sung, J.H., Yang, J.M., Park, S.B., Kwak, S.J., Park, J.S., 2007. Wound healing effect of adipose-derived stem cells: a critical role of secretory factors on human dermal fibroblasts. *J. Dermatol. Sci.* 48 (1), 15–24.
- Kim, J.E., Woo, Y.J., Sohn, K.M., Jeong, K.H., Kang, H., 2017. Wnt/ β -catenin and ERK pathway activation: a possible mechanism of photobiomodulation therapy with light-emitting diodes that regulate the proliferation of human outer root sheath cells. *Laser Surg. Med.* 49 (10), 940–947.
- Lev-Tov, H., Mamalis, A., Brody, N., Siegel, D., Jagdeo, J., 2013. Inhibition of fibroblast proliferation in vitro using red light-emitting diodes. *Dermatol. Surg.* 39 (8), 1167–1170.
- Lucke, L.D., Bortolazzo, F.O., Theodoro, V., Fujii, L., Bombeiro, A.L., Felonato, M., Dalia, R.A., Carneiro, G.D., Cartarozzi, L.P., Vicente, C.P., Oliveira, A.L.R., Mendonça, F.A.S., Esquisatto, M.A.M., Pimentel, E.R., de Aro, A.A., 2019. Low-level laser and adipose-derived stem cells altered remodelling genes expression and improved collagen reorganization during tendon repair. *Cell Prolif* 52 (3), e12580.
- Mahl, C., Egea, V., Megens, R.T., Pitsch, T., Santovito, D., Weber, C., Ries, C., 2016. RECK (reversion-inducing cysteine-rich protein with Kazal motifs) regulates migration, differentiation and Wnt/ β -catenin signaling in human mesenchymal stem cells. *Cell. Mol. Life Sci.* 73 (7), 1489–1501.
- Mamalis, A., Jagdeo, J., 2017. The combination of resveratrol and high-fluence light emitting diode-red light produces synergistic photobioinhibition of fibroblast proliferation and collagen synthesis: a novel treatment for skin fibrosis. *Dermatol. Surg.* 43 (1), 81–86.
- Mamalis, A., Garcha, M., Jagdeo, J., 2015a. Light emitting diode-generated blue light modulates fibrosis characteristics: fibroblast proliferation, migration speed, and reactive oxygen species generation. *Laser Surg. Med.* 47 (2), 210–215.
- Mamalis, A., Koo, E., Isseroff, R.R., Murphy, W., Jagdeo, J., 2015b. Resveratrol prevents high fluence red light-emitting diode reactive oxygen species-mediated photoinhibition of human skin fibroblast migration. *PLoS One* 10 (10), e0140628.
- Mamalis, A., Siegel, D., Jagdeo, J., 2016a. Visible red light emitting diode photobiomodulation for skin fibrosis: key molecular pathways. *Curr Dermatol Rep* 5, 121–128.
- Mamalis, A., Koo, E., Garcha, M., Murphy, W.J., Isseroff, R.R., Jagdeo, J., 2016b. High fluence light emitting diode-generated red light modulates characteristics associated with skin fibrosis. *J. Biophot.* 9 (11–12), 1167–1179.
- Martignago, C.C.S., Tim, C.R., Assis, L., Da Silva, V.R., Santos, E.C.B.D., Vieira, F.N., Parizotto, N.A., Liebano, R.E., 2019. Effects of red and near-infrared LED light therapy on full-thickness skin graft in rats. *Laser Med. Sci.* 35 (1), 157–164.
- Mazini, L., Rochette, L., Amine, M., Malka, G., 2019. Regenerative capacity of adipose derived stem cells (ADSCs), comparison with mesenchymal stem cells (MSCs). *Int. J. Mol. Sci.* 20 (10).
- Moon, K.M., Park, Y.H., Lee, J.S., Chae, Y.B., Kim, M.M., Kim, D.S., Kim, B.W., Nam, S.W., Lee, J.H., 2012. The effect of secretory factors of adipose-derived stem cells on human keratinocytes. *Int. J. Mol. Sci.* 13 (1), 1239–1257.
- Morikawa, M., Derynck, R., Miyazono, K., 2016. TGF- β and the TGF- β family: context-dependent roles in cell and tissue physiology. *Cold Spring Harb. Perspect. Biol.* 8 (5).
- Nascimento, L.D.E.S., Nascimento, K.F.E.S., Pessoa, D.R., Nicolau, R.A., 2019. Effects of therapy with light emitting diode (LED) in the calcaneal tendon lesions of rats: a literature review. *Sci. World J.* 2019, 6043019.
- Oh, P.S., Kim, H.S., Kim, E.M., Hwang, H., Ryu, H.H., Lim, S., Sohn, M.H., Jeong, H.J., 2017. Inhibitory effect of blue light emitting diode on migration and invasion of cancer cells. *J. Cell. Physiol.* 232 (12), 3444–3453.
- Oliveira, F.A., Matos, A.A., Santesso, M.R., Tokuhara, C.K., Leite, A.L., Bagnato, V.S., Machado, M.A., Peres-Buzalaf, C., Oliveira, R.C., 2016. Low intensity lasers differently induce primary human osteoblast proliferation and differentiation. *J. Photochem. Photobiol.* B 163, 14–21.
- Ong, W.K., Chen, H.F., Tsai, C.T., Fu, Y.J., Wong, Y.S., Yen, D.J., Chang, T.H., Huang, H.D., Lee, O.K., Chien, S., Ho, J.H., 2013. The activation of directional stem cell motility by green light-emitting diode irradiation. *Biomaterials* 34 (8), 1911–1920.
- Paganelli, A., Benassi, L., Rossi, E., Magnoni, C., 2020. Extracellular matrix deposition by adipose-derived stem cells and fibroblasts: a comparative study. *Arch. Dermatol. Res.* 312 (4), 295–299.
- Peng, F., Wu, H., Zheng, Y., Xu, X., Yu, J., 2012. The effect of noncoherent red light irradiation on proliferation and osteogenic differentiation of bone marrow mesenchymal stem cells. *Laser Med. Sci.* 27 (3), 645–653.
- Phillips, C.J., Humphreys, I., Fletcher, J., Harding, K., Chamberlain, G., Macey, S., 2016. Estimating the costs associated with the management of patients with chronic wounds using linked routine data. *Int. Wound J.* 13, 1193–1197.
- Prakash, T.V., Chaudhary, D.R.A., Purushothaman, S., Smitha, K.V., Varada Arvind, K., 2016. Epidermal grafting for chronic complex wounds in India: a case series. *Cureus* 8 (3), e516.
- Priglinger, E., Maier, J., Chaudary, S., Lindner, C., Wurzer, C., Rieger, S., Redl, H., Wolbank, S., Dungal, P., 2018. Photobiomodulation of freshly isolated human adipose tissue-derived stromal vascular fraction cells by pulsed light-emitting diodes for direct clinical application. *J. Tissue Eng. Regen. Med.* 12 (6), 1352–1362.
- Prindeze, N.J., Moffatt, L.T., Shupp, J.W., 2012. Mechanisms of action for light therapy: a review of molecular interactions. *Exp. Biol. Med.* 237 (11), 1241–1248.
- Proffen, B.L., Haslauer, C.M., Harris, C.E., Murray, M.M., 2013. Mesenchymal stem cells from the retroperitoneal fat pad and peripheral blood stimulate ACL fibroblast migration, proliferation, and collagen gene expression. *Connect. Tissue Res.* 54 (1), 14–21.
- Roering, J.W., Weigand, A., Pfulmann, R., Horch, R.E., Beier, J.P., Boos, A.M., 2018. Mesenchymal stem cells promote lymphangiogenic properties of lymphatic endothelial cells. *J. Cell Mol. Med.* 22, 3740–3750.
- Sassoli, C., Chellini, F., Squecco, R., Tani, A., Idrizaj, E., Nosi, D., Giannelli, M., Zecchi-Orlandini, S., 2016. Low intensity 635nm diode laser irradiation inhibits fibroblast-myofibroblast transition reducing TRPC1 channel expression/activity: new perspectives for tissue fibrosis treatment. *Laser Surg. Med.* 48 (3), 318–332.
- Schneider, P.R., Buhrmann, C., Mobasher, A., Matis, U., Shakibaei, M., 2011. Three-dimensional high-density co-culture with primary tenocytes induces tenogenic differentiation in mesenchymal stem cells. *J. Orthop. Res.* 29 (9), 1351–1360.
- Shukunami, C., Takimoto, A., Oro, M., Hiraki, Y., 2006. Scleraxis positively regulates the expression of tenomodulin, a differentiation marker of tenocytes. *Dev. Biol.* 298 (1), 234–247.
- Tafilinski, L., Demir, E., Kauczok, J., Fuchs, P.C., Born, M., Suschek, C.V., Opländer, C., 2014. Blue light inhibits transforming growth factor- β -induced myofibroblast differentiation of human dermal fibroblasts. *Exp. Dermatol.* 23 (4), 240–246.
- Teuschl, A., Balmayor, E.R., Redl, H., van Griensven, M., Dungal, P., 2015. Phototherapy with LED light modulates healing processes in an in vitro scratch-wound model using 3 different cell types. *Dermatol. Surg.* 41 (2), 261–268.
- Vinck, E.M., Cagnie, B.J., Cornelissen, M.J., Declercq, H.A., Cambier, D.C., 2003. Increased fibroblast proliferation induced by light emitting diode and low power laser irradiation. *Laser Med. Sci.* 18 (2), 95–99.
- Volpato, L.E., de Oliveira, R.C., Espinosa, M.M., Bagnato, V.S., Machado, M.A., 2011. Viability of fibroblasts cultured under nutritional stress irradiated with red laser, infrared laser, and red light-emitting diode. *J. Biomed. Opt.* 16 (7), 075004.
- Wang, P.H., Huang, B.S., Horng, H.C., Yeh, C.C., Chen, Y.J., 2018. Wound healing. *J. Chin. Med. Assoc.* 81 (2), 94–101.
- Winer, J., Jung, C.K., Shackel, I., Williams, P.M., 1999. Development and validation of real-time quantitative reverse transcriptase-polymerase chain reaction for monitoring gene expression in cardiac myocytes in vitro. *Anal. Biochem.* 270 (1), 41–49.
- Yang, X., Meng, H., Quan, Q., Peng, J., Lu, S., Wang, A., 2018. Management of acute Achilles tendon ruptures: a review. *Bone Joint Res.* 7 (10), 561–569.
- Yang, X.F., He, X., He, J., Zhang, L.H., Su, X.J., Dong, Z.Y., Xu, Y.J., Li, Y., Li, Y.L., 2011. High efficient isolation and systematic identification of human adipose-derived mesenchymal stem cells. *J. Biomed. Sci.* 18, 59.

- Yeh, N.G., Wu, C.-H., Cheng, C.T., 2010. Light-emitting diodes – their potential in biomedical applications. *Renew. Sustain. Energy Rev.* 14 (8), 2161–2166.
- Yoshino, P., Nishiyama, C.K., Modena, K.C., Santos, C.F., Sipert, C.R., 2013. In vitro cytotoxicity of white MTA, MTA Fillapex® and Portland cement on human periodontalligament fibroblasts. *Braz. Dent. J.* 24 (2), 111–116.
- Zhang, L., Xiong, Z., Li, Z., Yao, B., Zhang, D., 2009. Effects of red light emitting diode on apoptosis of HeLa cells and suppression of implanted HeLa cells growth in mice. *J. Radiat. Res.* 50 (2), 109–117.
- Zhao, J., Hu, L., Liu, J., Gong, N., Chen, L., 2013. The effects of cytokines in adipose stem cell-conditioned medium on the migration and proliferation of skin fibroblasts in vitro. *BioMed Res. Int.* 2013, 578479.
- Zheng, Z., James, A.W., Li, C., Jiang, W., Wang, J.Z., Chang, G.X., Lee, K.S., Chen, F., Berthiaume, E.A., Chen, Y., Pan, H.C., Chen, E.C., Li, W., Zhao, Z., Zhang, X., Ting, K., Soo, C., 2017. Fibromodulin reduces scar formation in adult cutaneous wounds by eliciting a fetal-like phenotype. *Signal Transduct. Target Ther.* 2, 17050.